Ultra-wideband Optical Receiver Using Electrical Spectrum Decomposition Technique

F. Hamaoka[(1)], M. Nakamura[(1)], M. Nagatani[(1, 2)], H. Wakita[(2)], T. Kobayashi[(1)], H. Yamazaki[(1, 2)], H. Nosaka[(1, 2)], and Y. Miyamoto[(1)]

[(1)] NTT Network Innovation Labs, NTT Corporation, 1-1 Hikarinooka, Yokosuka, Japan
fukutaro.hamaoka.xz@hco.ntt.co.jp
[(2)] NTT Device Technology Labs, NTT Corporation, 3-1 Morinosato-Wakamiya, Atsugi, Japan

Abstract *We propose an electrical spectrum decomposition technique using an ultra-broadband electrical bandwidth divider consisting of newly developed AMUX-based frequency shifters and an adder-subtractor based on in-house InP-HBT technology. Ultra-wideband optical 2×56-GBaud QPSK signal was successfully received and decomposed into narrowband signals.*

Introduction

Much research focuses on ultra-wideband signal -handling techniques to increase the transmission capacity per fibre while reducing the cost per bit of optical transmission systems.

At the transmitter side, several techniques for electrically composing low-speed signals into a high-speed signal have recently been proposed to generate the 100- and 200-GBaud-class high-speed ultra-broadband signals [1–5] to overcome the bandwidth limitation of digital-to-analogue convertors (DACs). For example, it has been demonstrated that a 100-GHz DAC based on a digital bandwidth interleaving technique using microwave mixers [2] and 192-GBaud quadrature phase shift keying (QPSK) signal generation using the ultra-broadband analogue-multiplexer (AMUX) integrated optical frontend module [5].

Recently, at the receiver side, an analogue 1-to-4 demultiplexer in a SiGe heterojunction bipolar transistor (HBT) BiCMOS has been proposed to overcome the bandwidth limitation of analogue-to-digital convertors (ADCs) [6]. The 1-to-4 ADC frontend enabled 100-GBaud PAM4 signal reception with an ADC bandwidth of 14 GHz.

In this study, we propose an ultra-wideband optical receiver configuration based on an electrical spectrum decomposition technique that converts an ultra-wideband signal to narrowband signals. The proposed electrical spectrum decomposition technique uses an ultra-broadband electrical bandwidth divider consisting of newly developed frequency shifters and an adder-subtractor, which are based on in-house indium phosphide (InP) HBT technology [7]. A received ultra-wideband optical 2×56-GBaud QPSK signal was successfully decomposed into narrowband signals with the proposed technique.

Electrical spectrum decomposition technique

Figure 1 shows a schematic diagram of the ultra-wideband optical receiver configuration based on the proposed electrical spectrum decomposition technique.

An ultra-wideband signal can be divided into narrowband signals:

$$E = E_1 \exp(j\omega t) + E_2 \exp(-j\omega t)\,, \qquad (1)$$

where $E_1 \exp(j\omega t)$ and $E_2 \exp(-j\omega t)$ are respectively upper and lower sideband signals; $E(= I + jQ)$, $E_1\ (= I_1 + jQ_1)$ and $E_2\ (= I_2 + jQ_2)$ are respectively the baseband complex representation of the ultra-wideband and the narrowband upper and lower sideband signals; $\omega\ (= 2\pi f t)$ is an angular frequency; f is an

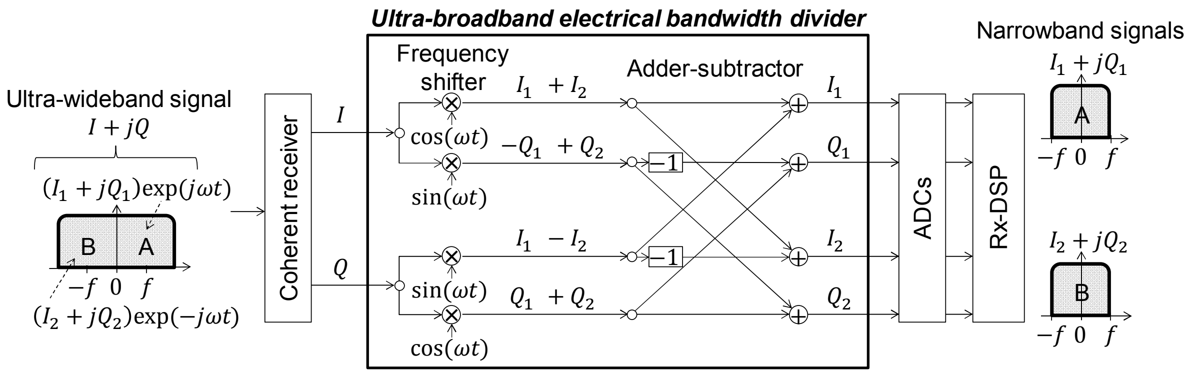

Fig. 1: Schematic of ultra-wideband optical receiver configuration based on electrical spectrum decomposition technique

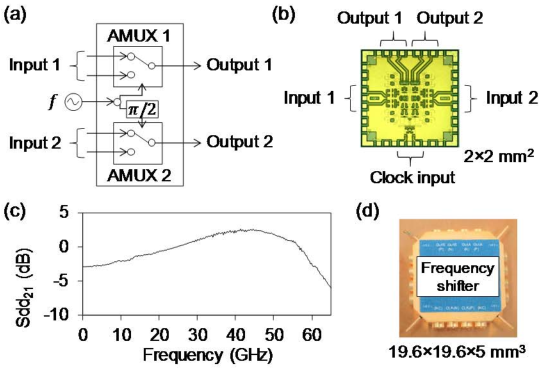

Fig. 2: Frequency Shifter: (a) functional block, (b) microphotograph of IC, (c) measured through-mode S-parameter of IC, and (d) photograph of module

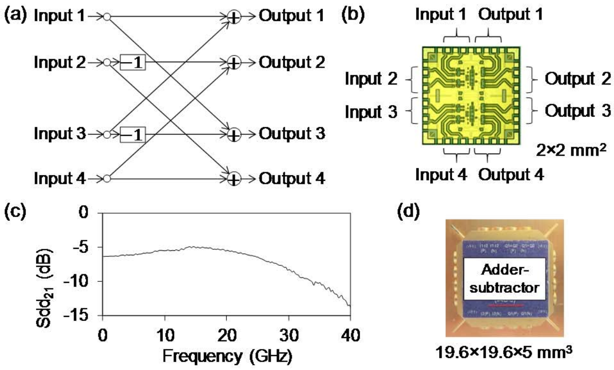

Fig. 3: Adder-subtractor: (a) functional block, (b) microphotograph of IC, (c) measured through-mode S-parameter of IC, and (d) photograph of module

intermediate frequency (IF); and j is an imaginary unit. Equation (1) is transformed as

$$E = (I_1 + I_2)\cos(\omega t) + (-Q_1 + Q_2)\sin(\omega t) + j[(I_1 - I_2)\sin(\omega t) + (Q_1 + Q_2)\cos(\omega t)]. \quad (2)$$

After detecting the optical ultra-wideband signal at a coherent receiver, an ultra-broadband electrical bandwidth divider, which consists of frequency shifters and an adder-subtractor, decomposes the ultra-wideband signal into the narrowband signals.

The frequency shifters down-convert the high-speed signal into baseband. Specifically, the frequency shifters multiply the in-phase (I) and the quadrature (Q) components of the ultra-wideband signal by $\cos(\omega t)$ or $\sin(\omega t)$:

$$I \times cos(\omega t) = \frac{1}{2}\{(I_1 + I_2) + (I_1 + I_2)\cos(2\omega t) + (-Q_1 + Q_2)\sin(2\omega t)\}, \quad (3)$$

$$I \times \sin(\omega t) = \frac{1}{2}\{(-Q_1 + Q_2) + (I_1 + I_2)\sin(2\omega t) + (Q_1 - Q_2)\cos(2\omega t)\}, \quad (4)$$

$$Q \times sin(\omega t) = \frac{1}{2}\{(I_1 - I_2) + (Q_1 + Q_2)\sin(2\omega t) + (-I_1 + I_2)\cos(2\omega t)\}, \quad (5)$$

$$Q \times cos(\omega t) = \frac{1}{2}\{(Q_1 + Q_2) + (Q_1 + Q_2)\cos(2\omega t) + (I_1 - I_2)\sin(2\omega t)\}, \quad (6)$$

where the first terms on the right side of Eqs. (3)–(6) are the down-converted narrowband signals, and the second and third terms are unnecessary harmonic components that can be removed by a low-pass filter or bandwidth-optimized ADC. After down-converting the ultra-wideband signals in the frequency sifters, the adder-subtractor decomposes the in-phase and quadrature components of down-converted narrowband signals as shown in Fig. 1. Finally, ADCs digitize the narrowband signals, and then a receiver-side (Rx) digital signal processing (DSP) demodulates the signals.

Frequency shifter and adder-subtractor for ultra-broadband electrical bandwidth divider

We have developed frequency shifter and adder-subtractor prototypes using in-house InP-HBT technology for constructing the ultra-broadband electrical bandwidth divider.

Figure 2 (a) shows the functional block of the frequency shifter, which consists of two AMUXs based on in-house InP-HBT technology. The two AMUXs are the same generation as that reported in [7]. The input clock is branched into two. Each clock is supplied to the AMUX with the phase difference of $\pi/2$ radian; each AMUX in the frequency shifter down-converts the input ultra-wideband signal to baseband signal with the clock phase difference. This achieves the same operation as in Eqs. (3)–(6), which multiplies the ultra-wideband signals by $\cos(\omega t)$ or $\sin(\omega t)$. Figure 2 (b) shows a microphotograph of the frequency shifter integrated circuit (IC) with a chip size of 2×2 mm^2. The frequency shifter IC consumes 0.99 W at a supply voltage of −4.5 V. The analogue output bandwidth of the frequency shifter IC is 64 GHz from the characteristics of a measured S-parameter Sdd$_{21}$ through input 1 to output 1 as shown in Fig. 2(c).

Figure 3 (a) shows the functional block of the adder-subtractor based on in-house InP-HBT technology. The down-converted signals are decomposed into the in-phase and quadrature components of the narrowband signals by addition and subtraction. Figure 3 (b) shows a microphotograph of the adder-subtractor IC with a chip size of 2×2 mm^2. The adder-subtractor IC consumes 0.52 W at a supply voltage of −4.0 V. The analogue input and output bandwidth of the adder-subtractor IC are designed to be 64 and 32 GHz, respectively. The adder-subtractor IC has the output bandwidth of 32 GHz from the measured S-parameter Sdd$_{21}$ through input 1 to

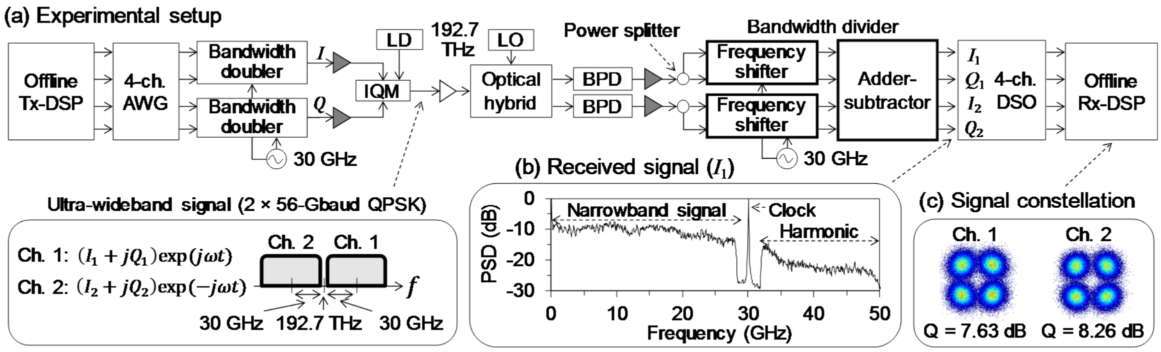

Fig. 4: (a) Experimental setup for demonstration of ultra-broadband optical receiver using proposed electrical spectrum decomposition technique, (b) PSD of received signal (I_1) and (c) signal constellation after applying offline RX-DSP

output 1 as shown in Fig.3(c).

Figures 2 (d) and 3 (d) show photographs of the frequency shifter and adder-subtractor modules. Each IC is installed in the newly developed ultra-low-loss metal package in which the 16-port G3PO (SMPS) connectors are introduced. The package size is as small as 19.6×19.6×5 mm^3.

Experimental setup and results

To demonstrate an ultra-wideband optical receiver, we received an ultra-wideband optical 2×56-GBaud QPSK signal with the electrical spectrum decomposition technique. Figure 4 (a) shows the experimental setup. This experiment was conducted in a back-to-back configuration using a single-polarization signal because of the limited number of prototypes of the frequency shifter and adder-subtractor.

At the transmitter side, the ultra-wideband optical 2×56-GBaud QPSK signal was generated in the ultra-wideband optical transmitter on the basis of our previously proposed electrical spectrum synthesis technique [4]. The transmitter consists of an offline transmitter-side (Tx) DSP, a 4-channel arbitrary waveform generator (AWG) that functioned as a DAC at a sampling rate of 96 Gsamples/s and a bandwidth of 32 GHz, our InP-HBT AMUX-based bandwidth doublers with the IF clocks of 30 GHz, 60-GHz bandwidth drivers, and an optical lithium niobate IQ modulator (IQM). The optical carrier frequency of the 2×56-GBaud QPSK signal was 192.7 THz.

At the receiver side, the 2×56-GBaud QPSK signal amplified by an erbium doped fibre amplifier (EDFA) was received by a coherent receiver consisting of an optical hybrid and two balanced photodiodes (BPDs) with a bandwidth of 70 GHz. The centre frequency of the optical local oscillator (LO) input into the receiver was set to 192.7 THz. Each received signal of in-phase and quadrature components amplified by the 67-GHz bandwidth driver was split into two signals by a power splitter. The ultra-broadband electrical bandwidth divider consisted of our newly developed frequency shifters and adder-subtractor. The frequency shifters with the IF clocks of 30-GHz down-converted the received ultra-wideband signals from the power splitters to baseband signals. Then, the adder-subtractor decomposed the baseband signals into in-phase and quadrature components of the narrowband signals. A digital-storage oscilloscope (DSO) with a bandwidth of 100 GHz digitized the received signal at a sampling rate of 256 Gsamples/s. The Rx-DSP was performed offline. The received signal was resampled at a rate of 2 samples/symbol. Signal equalization was achieved by T/2-spaced real-valued 4×4 adaptive finite impulse response filters enabling precise lane-by-lane equalization. The carrier-frequency offset and phase noise were compensated for by a digital phase-locked loop. Finally, we measured the bit error rate to calculate the Q-factor of the received signal.

Figure 4 (b) shows the power spectral density (PSD) of the received signal I_1 (in-phase component of channel 1) after digitizing at the DSO. Our bandwidth divider enabled down-conversion of the ultra-wideband signal to narrowband signal. Figure 4 (c) shows signal constellations of channels 1 and 2 of the 2×56-GBaud QPSK signal. The Q-factors of channels 1 and 2 were 7.63 and 8.26 dB, respectively. The electrical spectrum decomposition technique successfully decomposed the ultra-wideband 2×56-GBaud QPSK signal.

Conclusions

We proposed an electrical spectrum decomposition technique using an ultra-broadband electrical bandwidth divider consisting of newly developed AMUX-based frequency shifters and an adder-subtractor based on in-house InP-HBT technology. As a demonstration of an ultra-broadband optical receiver, an ultra-wideband optical 2×56-GBaud QPSK signal was successfully received and decomposed into narrowband signals using the proposed technique.

References

[1] H. Yamazaki et al., “160-Gbps Nyquist PAM4 transmitter using a digital-preprocessed analog-multiplexed DAC”, ECOC2015, Valencia, Spain, Sep. 2015, PDP.2.2.

[2] X. Chen et al., “All-electronic 100-GHz bandwidth digital-to-analog converter generating PAM signals up to 190-GBaud”, OFC2016, Anaheim, CA, USA, Mar. 2016, Th5C.5.

[3] G. Raybon et al., “180-GBaud all-ETDM single-carrier polarization multiplexed QPSK transmission over 4480 km”, OFC2018, San Diego, CA, USA, Mar. 2018, Th4C.3.

[4] F. Hamaoka et al., “Electrical spectrum synthesis technique using digital pre-processing and ultra-broadband electrical bandwidth doubler for high-speed optical transmitter”, Electron Lett., vol. 54, no. 24, pp. 1390–1391, 2018.

[5] M. Nakamura et al., “192-Gbaud signal generation using ultra-broadband optical frontend module integrated with bandwidth multiplexing function”, OFC2019, San Diego, CA, USA, Mar. 2019, Th4B.4.

[6] F. Buchali et al., “A SiGe HBT BiCMOS 1-to-4 ADC frontend supporting 100 GBaud PAM4 reception at 14 GHz digitizer bandwidth”, OFC2019, San Diego, CA, USA, Mar. 2019, Th4A.7.

[7] M. Nagatani et al., “A 128-GS/s 63-GHz-bandwidth InP-HBT-based analog-MUX module for ultra-broadband D/A conversion subsystem”, IMS2017, Honololu, HI, USA, June 2017, TU2H-2.